Mineralogy and Petrology
https://doi.org/10.1007/s00710-022-00803-0

RESEARCH

Nishanbaevite, $KAl_2O(AsO_4)(SO_4)$, a new As/S-ordered arsenate-sulfate mineral of fumarolic origin

Igor V. Pekov[1] · Natalia V. Zubkova[1] · Vasiliy O. Yapaskurt[1] · Dmitry I. Belakovskiy[2] · Sergey N. Britvin[3] · Atali A. Agakhanov[2] · Anna G. Turchkova[1] · Evgeny G. Sidorov[4] · Anton V. Kutyrev[4] · Vladislav A. Blatov[5] · Dmitry Y. Pushcharovsky[1]

Received: 20 September 2022 / Accepted: 23 November 2022

Abstract
The new mineral nishanbaevite, ideally $KAl_2O(AsO_4)(SO_4)$, was found in sublimates of the Arsenatnaya fumarole at the Second scoria cone of the Northern Breakthrough of the Great Tolbachik Fissure Eruption, Tolbachik volcano, Kamchatka, Russia. It is associated with euchlorine, alumoklyuchevskite, langbeinite, urusovite, lammerite, lammerite-β, ericlaxmanite, kozyrevskite, and hematite. Nishanbaevite occurs as long-prismatic or lamellar crystals up to 0.03 mm typically combined in brush-like aggregates and crusts up to 1.5 mm across. It is transparent, colourless, with vitreous lustre. D_{calc} = 3.012 g cm^{-3}. Nishanbaevite is optically biaxial (–), $\alpha = 1.552$, $\beta \approx \gamma = 1.567$. The chemical composition (average of seven analyses) is: Na_2O 3.79, K_2O 8.01, CaO 0.10, CuO 0.21, Al_2O_3 30.08, Fe_2O_3 0.50, SiO_2 1.62, P_2O_5 0.66, As_2O_5 32.23, SO_3 22.59, total 99.79 wt%. The empirical formula calculated based on 9 O *apfu* is: $(K_{0.57}Na_{0.41}Ca_{0.01})_{\Sigma 0.99}(Al_{1.99}Fe^{3+}_{0.02}Cu_{0.01})_{\Sigma 2.02}(As_{0.95}S_{0.95}Si_{0.09}P_{0.03})_{\Sigma 2.02}O_9$. Nishanbaevite is orthorhombic, *Pbcm*, $a = 15.487(3)$, $b = 7.2582(16)$, $c = 6.6014(17)$ Å, $V = 742.1(3)$ Å^3 and $Z = 4$. The strongest reflections of the powder XRD pattern [*d*,Å(*I*)(*hkl*)] are: 15.49(100)(100), 6.56(30)(110), 4.653(29)(111), 3.881(54)(400), 3.298(52)(002), 3.113(29)(121), and 3.038(51)(202, 411). The crystal structure, solved from single-crystal XRD data ($R = 7.58\%$), is unique. It is based on the complex heteropolyhedral sheets formed by zig-zag chains of Al-centred polyhedra (alternating trigonal bipyramids AlO_5 and octahedra AlO_6 sharing edges) and isolated tetrahedra AsO_4 and SO_4. Adjacent chains of Al polyhedra are connected *via* AsO_4 tetrahedra to form a heteropolyhedral double-layer. Its topological peculiarity is considered and compared with those in structurally related compounds. The (K,Na) site is located in the interlayer space between SO_4 tetrahedra. The position of nishanbaevite among the arsenate-sulfates and their specific structural features are discussed. The mineral is named in honour of the Russian mineralogist Tursun Prnazorovich Nishanbaev (1955–2017).

Keywords Nishanbaevite · New mineral · Potassium aluminium arsenate sulfate · Crystal structure · Fumarole · Tolbachik volcano · Kamchatka

Editorial handling: G. Giester

✉ Igor V. Pekov
igorpekov@mail.ru

[1] Faculty of Geology, Moscow State University, Vorobievy Gory, 119991 Moscow, Russia

[2] Fersman Mineralogical Museum of the Russian Academy of Sciences, Leninsky Prospekt 18-2, 119071 Moscow, Russia

[3] St. Petersburg State University, University Emb. 7/9, 199034 St. Petersburg, Russia

[4] Institute of Volcanology and Seismology, Far Eastern Branch of Russian Academy of Sciences, Piip Boulevard 9, 683006 Petropavlovsk-Kamchatsky, Russia

[5] Samara Center for Theoretical Materials Science (SCTMS), Samara State Technical University, Molodogvardeyskaya St. 244, 443100 Samara, Russia

Published online: 09 December 2022

Introduction

Natural sulfates and arsenates are numerous: altogether, about 800 valid mineral species belonging to these chemical classes are known. Sulfate and arsenate minerals are especially common and diverse in the oxidation zone of ore deposits where they occur in significant amounts and form close associations with each other. At the same time, arsenate-sulfates, the mixed oxysalts with both SO_4 and AsO_4 as species-defining anions are few: twenty-one mineral species. Among them, only beudantite $PbFe^{3+}{}_3(AsO_4)(SO_4)_2(OH)_6$ can be considered as a relatively common mineral. A brief review of these minerals, including data on As-S order/disorder in their structures was reported by Pekov et al. (2021). Nineteen arsenate-sulfate minerals contain OH groups or/and H_2O molecules and have supergene or low-temperature hydrothermal origin whilst two species are H-free, namely vasilseverginite $Cu_9O_4(AsO_4)_2(SO_4)_2$ and as described in this paper nishanbaevite $KAl_2O(AsO_4)(SO_4)$. Both these minerals, as well as a single natural H-free phosphate-sulfate, karlditmarite $Cu_9O_4(PO_4)_2(SO_4)_2$ (Siidra et al. 2021), are found only in high-temperature sublimates of the Arsenatnaya fumarole at the Tolbachik volcano, Kamchatka, Russia.

The new mineral nishanbaevite (Cyrillic: нишанбаевит) is named in honour of the Russian mineralogist Tursun Prnazorovich Nishanbaev (1955–2017), a Head of the Natural History Museum of the Ilmen Natural Reserve, Miass, Russia. Dr. Nishanbaev made a significant contribution to the mineralogy of anthropogene counterparts of volcanic fumaroles which originate on burning dumps of coal mines.

Both the new mineral and its name have been approved by the IMA Commission on New Minerals, Nomenclature and Classification (IMA2019–012). The type specimen is deposited in the systematic collection of the Fersman Mineralogical Museum of the Russian Academy of Sciences, Moscow with the catalogue number 96592.

Occurrence

Nishanbaevite was detected in the single specimen collected by us in July 2015 from the Arsenatnaya fumarole located at the apical part of the Second scoria cone of the Northern Breakthrough of the Great Tolbachik Fissure Eruption (GTFE), Tolbachik volcano, Kamchatka Peninsula, Far-Eastern Region, Russia (55°41'N 160°14'E, 1200 m asl). This scoria cone is a monogenetic volcano about 300 m high and approximately 0.1 km^3 in volume. It was formed in 1975 during the first phase of the GTFE (Fedotov and Markhinin 1983). Fumarole fields at the Second scoria cone are still active; gas vents with temperatures up to 500 °C are numerous at the summit of the cone. The active, hot Arsenatnaya fumarole, first uncovered by us in July 2012, belongs to oxidizing-type fumaroles and is one of the world's most prolific mineralogical occurrences of the volcanic exhalation origin: for this decade, two hundred mineral species, mainly sulfates and arsenates, are found here, including 64 IMA-approved new minerals. The Arsenatnaya fumarole and its mineralogical features, including zonation in the distribution of mineral associations, were characterized by Pekov et al. (2014, 2018) and Shchipalkina et al. (2020).

Nishanbaevite was found in a pocket about 1.3 m below the day surface, within the upper part the so-called polymineralic zone of the fumarole (zone IV: Shchipalkina et al. 2020). The temperatures measured by us using a chromel-alumel thermocouple in this area during sampling were 380–400 °C. Walls of the pocket were covered by sublimate incrustations with dominating euchlorine. Other minerals associated with nishanbaevite are alumoklyuchevskite, langbeinite, urusovite, lammerite, lammerite-β, ericlaxmanite, kozyrevskite and hematite.

Nishanbaevite could be deposited directly from the gas phase as a volcanic sublimate or, more probably, it was formed as a result of the interaction between fumarolic gas and basalt scoria at the temperatures not lower than 400 °C. The latter could be a source of Al which has low volatility in such post-volcanic systems at temperatures up to 400–500 °C (Symonds and Reed 1993).

General appearance, physical properties and optical data

Nishanbaevite occurs as long-prismatic, typically lath-like crystals up to $0.01 \times 0.01 \times 0.05$ mm^3, or lamellar crystals up to 0.02 mm × 0.03 mm and less than 1 μm thick. Some crystals observed under the scanning electron microscope (SEM) demonstrate signs of X-shaped interpenetration twins (Fig. 1), however, the twin law was not determined. The crystals are combined in clusters which form brush-like, openwork aggregates (Fig. 1) up to 0.5 mm across and crusts up to 1.5 mm across (Fig. 2). They overgrow incrustations of langbeinite, alumoklyuchevskite, or hematite or occur on the surface of basalt scoria altered by fumarolic gas.

The mineral is transparent, colourless in individuals and snow-white in aggregates (Fig. 2), with a white streak and a vitreous lustre. It is non-fluorescent under ultraviolet light or an electron beam. Nishanbaevite is brittle, cleavage or parting was not observed and the fracture is uneven (observed under the microscope). Density calculated using the empirical formula and unit-cell volume found from single-crystal X-ray diffraction data is 3.012 g cm^{-3}.

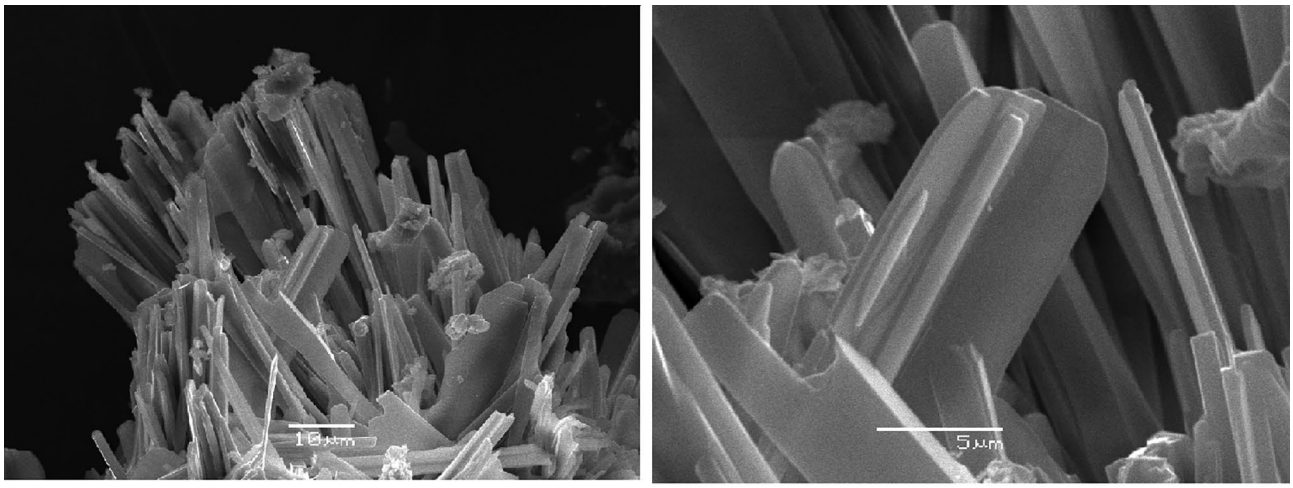

Fig. 1 Typical cluster of nishanbaevite crystals (**a**) and its magnified fragment (**b**). SEM images, secondary electron mode

Nishanbaevite is optically biaxial (–), $\alpha = 1.552(2)$, $\gamma = 1.567(2)$ (589 nm); β was not precisely determined, it is close to γ. $2V_{meas}$ is small. Extinction is straight and elongation is positive. Dispersion of optical axes was not observed. In plane-polarized light, the mineral is colourless and non-pleochroic.

Chemical composition

The chemical data for nishanbaevite were obtained using electron probe micro-analysis (EPMA). A Jeol JSM-6480LV scanning electron microscope equipped with an INCA-Wave 500 wavelength-dispersive spectrometer was used, with an acceleration voltage of 20 kV, a beam current of 20 nA, and a 3 μm beam diameter. The following natural and synthetic reference materials and the following analytical lines were used: jadeite (Na *K*α, Al *K*α, Si *K*α), $KTiOPO_4$ (K *K*α, P *K*α), $CaSiO_3$ (Ca *K*α), CuO (Cu *K*α), FeS_2 (Fe *K*α), GaAs (As *L*α), and ZnS (S *K*α). Peak and background counting times are 20 and (10 + 10) s, respectively. Contents of other elements with atomic numbers > 6 are below their detection limits.

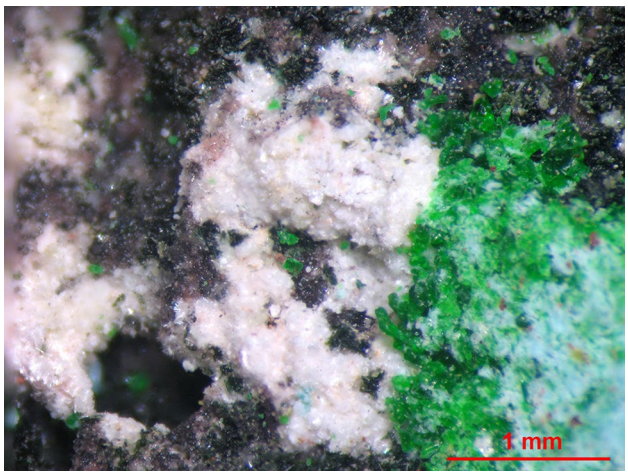

Fig. 2 Snow-white crusts of nishanbaevite crystals with bright green euchlorine, bluish fine-grained lammerite and iron-black hematite overgrowing reddish-brown basalt scoria altered by fumarolic gas. Photo: I.V. Pekov & A.V. Kasatkin

The chemical composition of nishanbaevite (average of seven spot analyses, wt%, range / standard deviations are in parentheses) is: Na_2O 3.79 (3.01–4.39 / 0.55), K_2O 8.01 (6.90–9.06 / 0.77), CaO 0.10 (0.02–0.22 / 0.08), CuO 0.21 (0.04–0.44 / 0.14), Al_2O_3 30.08 (26.63–32.40 / 2.29), Fe_2O_3 0.50 (0.31–0.67 / 0.12), SiO_2 1.62 (0.84–4.97 / 1.50), P_2O_5 0.66 (0.60–0.72 / 0.04), As_2O_5 32.23 (28.48–36.99 / 3.28), SO_3 22.59 (21.68–23.57 / 0.62), total 99.79. Trivalent state of admixed iron is assumed because of strongly oxidizing conditions of mineral formation in the Arsenatnaya fumarole: all iron minerals known here contain only Fe^{3+} (Pekov et al. 2018; Shchipalkina et al. 2020).

The empirical formula calculated on the basis of 9 O atoms per formula unit is $(K_{0.57}Na_{0.41}Ca_{0.01})_{\Sigma 0.99}(Al_{1.99}Fe^{3+}_{0.02}Cu_{0.01})_{\Sigma 2.02}(As_{0.95}S_{0.95}Si_{0.09}P_{0.03})_{\Sigma 2.02}O_9$. The simplified formula is $(K,Na)Al_2O(AsO_4)(SO_4)$ and the idealised, end-member formula is $KAl_2O(AsO_4)(SO_4)$, which requires K_2O 13.69, Al_2O_3 29.64, As_2O_5 33.40, SO_3 23.27, total 100 wt%.

X-ray crystallography and crystal structure determination

Powder X-ray diffraction (XRD) data of nishanbaevite (Table 1) were collected with a Rigaku R-AXIS Rapid II single-crystal diffractometer equipped with cylindrical

image plate detector ($r = 127.4$ mm) using Debye-Scherrer geometry, Co$K\alpha$ radiation (rotating anode with VariMAX microfocus optics), 40 kV, 15 mA, and 12 min exposure. Angular resolution of the detector is 0.045 2Θ (pixel size 0.1 mm). The data were integrated using the software package osc2Tab (Britvin et al. 2017). The orthorhombic unit cell parameters refined from the powder data are: $a = 15.505(5)$, $b = 7.257(2)$, $c = 6.606(2)$ Å, and $V = 743.3(6)$ Å^3.

Single-crystal XRD studies of nishanbaevite were carried out using an Xcalibur S diffractometer equipped with a CCD (charge-coupled device) detector. More than a hemisphere of three-dimensional data was collected. Data reduction was performed using CrysAlisPro Version 1.171.37.34 (Agilent Technologies 2014). The data were corrected for Lorentz factor and polarization effects. The crystal structure was solved by direct methods and refined using the SHELX software package (Sheldrick 2015) to $R = 0.0758$ for 547 unique reflections with $I > 2\sigma(I)$. Crystal data, data collection information and structure refinement details are given in Table 2, coordinates and thermal displacement parameters of atoms in Table 3, selected interatomic distances in Table 4 and bond valence calculations in Table 5.

Unfortunately, even the best of tested crystals of nishanbaevite was not perfect and very small that caused rather low-quality diffraction data. However, the reasonable values of interatomic distances (Table 4) and bond valence sums (Table 5), as well as very good agreement between the measured and calculated powder XRD patterns (Table 1) show that the structure is determined correctly.

Discussion

The crystal structure of nishanbaevite (Fig. 3) is unique. It is based on the complex heteropolyhedral (100) double layers formed by zig-zag [001] chains of Al-centred polyhedra and isolated from each other AsO_4 and SO_4 tetrahedra. Within these layers two symmetrically equivalent single sheets are connected by the gliding plane *b*. There are two crystallographically non-equivalent Al sites which centre alternating $Al(1)O_5$ trigonal bipyramids and $Al(2)O_6$ octahedra sharing edges to form the chains (Fig. 3a). Adjacent chains are connected *via* AsO_4 tetrahedra sharing common vertices with Al-centred polyhedra and thus forming double-layered core of the heteropolyhedral sheet. Each tetrahedron shares three vertices with the chains of one layer of the core (Fig. 4) and one vertex with the chains of the second one. SO_4 tetrahedra are linked to the external parts of the double-layered core from both sides sharing two common vertices with $Al(2)O_6$ octahedra. The large-cation *A* site with disordered

Table 1 Powder X-ray diffraction data (*d* in Å) of nishanbaevite

I_{obs}	d_{obs}	I_{calc}*	d_{calc}**	*h k l*
100	**15.49**	100	15.487	100
30	**6.56**	28	6.572	110
6	5.295	6	5.296	210
2	5.172	1	5.162	300
29	**4.653**	23	4.658	111
21	4.212	21	4.207	310
54	**3.881**	48	3.872	400
27	3.625	30	3.629	020
15	3.548	12, 4	3.548, 3.533	311, 120
5	3.426	2	3.416	410
52	**3.298**	40, 7	3.301, 3.286	002, 220
3	3.175	3	3.180	021
29	**3.113**	28	3.115	121
51	**3.038**	21, 27	3.036, 3.034	202, 411
15	2.948	12, 2	2.950, 2.942	112, 221
10	2.800	8	2.801	212
1	2.706	2	2.708	321
19	2.650	22	2.648	420
5	2.590	1, 4	2.597, 2.581	312, 600
24	2.514	23	2.512	402
14	2.440	12	2.442	022
1	2.411	1	2.412	122
9	2.360	10	2.356	520
3	2.328	2	2.329	222
2	2.307	1	2.309	230
1	2.217	1	2.219	521
3	2.181	2	2.180	231
2	2.122	1	2.116	710
2	2.084	1	2.079	331
3	2.067	2	2.065	422
5	2.038	5	2.033	602
2	2.017	1	2.015	711
2	2.007	2	2.004	621
3	1.951	2	1.950	313
2	1.940	1, 1	1.936, 1.936	132, 800
3	1.908	5	1.907	530
5	1.881	4	1.882	023
6	1.869	6	1.868	123
2	1.852	2	1.850	413
7	1.825	9	1.825	332
6	1.805	6	1.800	811
5	1.777	2, 6	1.782, 1.774	712, 622
6	1.738	9	1.739	141
3	1.727	4	1.721	900
2	1.708	1, 2	1.708, 1.707	820, 241
11	1.650	13	1.650	004
4	1.636	3, 2, 1	1.640, 1.633, 1.632	722, 730, 613
2	1.610	3	1.608	523
4	1.557	5	1.557	632
2	1.537	2	1.536	314

Table 1 (continued)

I_{obs}	d_{obs}	I_{calc}*	d_{calc}**	*h k l*
6	1.520	4, 4	1.523, 1.518	541, 404
2	1.502	2	1.502	024
4	1.476	2, 2	1.476, 1.475	10.1.1, 224
1	1.450	2	1.448	641
4	1.428	4	1.425	813
7	1.401	2, 2, 6, 2	1.402, 1.402, 1.401, 1.400	930, 10.0.2, 424, 043
6	1.395	1, 5	1.395, 1.394	251, 143
1	1.367	1, 1	1.367, 1.366	351, 614
1	1.353	2	1.352	524

*For the calculated pattern, only reflections with intensities ≥ 1 are given; **for the unit-cell parameters calculated from single-crystal data; the strongest reflections are marked in bold type

distribution of K and subordinate Na is located in the interlayer space between SO_4 tetrahedra.

A topological analysis aimed with the search of the related compounds was performed with the program package *ToposPro* (Blatov et al. 2014). The 'Junction atoms' algorithm (Shevchenko and Blatov 2021) was used to simplify the nishanbaevite structure with the oxygen atoms as junctions; potassium/sodium atoms were excluded from the consideration at this step. As a result, the topological representation of nishanbaevite is consisted of centers of AlO_6, AlO_5, AsO_4 and SO_4 groups. The simplified double periodic layer is represented by a 6,6-coordinated net with AlO_6, AlO_5, AsO_4 groups as nodes and bridging SO_4 groups as links. The term "6,6-coordinated" means that the net contains two types of topologically different nodes with the number of contacts (coordination) equal to six. One type of node is represented by the AlO_6 groups, while AlO_5 and AsO_4 groups are topologically equivalent, i.e. they are equally connected to other groups, and they represent the other type of node. The specific feature of the node formed by AlO_6 is that it is bounded to all types of building units, namely AlO_6, AlO_5, AsO_4 and SO_4 and formally its coordination is equal to 8 (Fig. 5a). However, within the simplified net SO_4 groups are considered as edges and thus in such approach AlO_6 node is surrounded by 6 neighboring nodes. In contrast with it the coordination of AlO_5 and AsO_4 nodes is formed only by AlO_6, AlO_5 and AsO_4 groups located within the net. The difference between AlO_5 and AsO_4 is in the method of connecting to the six other

Table 2 Crystal data, data collection information and structure refinement details for nishanbaevite

Formula	$(K_{0.58}Na_{0.42})Al_2O[(As_{0.89}P'_{0.11})O_4][SO_4]$*
Formula weight	665.24
Temperature, K	293(2)
Radiation and wavelength, Å	Mo*K*α; 0.71073
Crystal system, space group, *Z*	Orthorhombic, *Pbcm*, 4
Unit cell dimensions, Å/°	$a = 15.487(3)$, $b = 7.2582(16)$, $c = 6.6014(17)$
V, Å^3	742.1(3)
Absorption coefficient μ, mm^{-1}	5.033
F_{000}	643
Crystal size, mm^3	0.01 × 0.01 × 0.02
Diffractometer	Xcalibur S CCD
Absorption correction	multi-scan Empirical absorption correction using spherical harmonics, implemented in SCALE3 ABSPACK scaling algorithm
θ range, °	3.10–25.24
Reflections collected	5583
Unique reflections	973 ($R_{int} = 0.1946$)
Unique reflections [$I > 2\sigma(I)$]	547
Structure solution	direct methods
Refinement method	full-matrix least-squares on F^2
Number of refined parameters	77
Final *R* indices [$I > 2\sigma(I)$]	$R1 = 0.0758$, w$R2 = 0.1261$
R indices (all data)	$R1 = 0.1506$, w$R2 = 0.1573$
GoF	1.054
Largest diff. peak and hole, e/Å^3	2.04 and − 1.46

*Relatively light elements (Si, S and P) which partially substitute As^{5+} in the As site are formally jointed as P' during refinement

Table 3 Atom coordinates and equivalent thermal displacement parameters (U_{eq}, in Å^2), site occupancy factors (s.o.f.) and site multiplicities (Q) for nishanbaevite

Site	*x*	*y*	*z*	U_{eq}	s.o.f.	*Q*
A	0.4117(4)	-0.0355(7)	0.25	0.051(2)	$K_{0.58(4)}Na_{0.42(4)}$	4
As	0.09601(10)	0.5610(2)	0.25	0.0113(5)	$As_{0.892(14)}P'_{0.108(14)}$*	4
S	0.3619(3)	0.0494(7)	0.75	0.0323(13)	$S_{1.00}$	4
Al(1)	0.1167(3)	0.4928(5)	0.75	0.0128(11)	$Al_{1.00}$	4
Al(2)	0.2233(3)	0.25	0.0	0.0152(11)	$Al_{1.00}$	4
O(1)	0.3073(5)	0.0733(9)	0.9326(10)	0.0232(19)	$O_{1.00}$	8
O(2)	0.1293(4)	0.4466(8)	0.4582(11)	0.0152(17)	$O_{1.00}$	8
O(3)	-0.0091(6)	0.5780(12)	0.25	0.021(3)	$O_{1.00}$	4
O(4)	0.2050(6)	0.3411(11)	0.75	0.011(2)**	$O_{1.00}$	4
O(5)	0.1358(6)	0.7727(12)	0.25	0.022(3)	$O_{1.00}$	4
O(6)	0.4256(8)	0.1954(19)	0.75	0.091(6)	$O_{1.00}$	4
O(7)	0.4002(10)	-0.1302(15)	0.75	0.088(6)	$O_{1.00}$	4

*P' = Si + S + P; ** U_{iso}

groups: AsO_4 uses for connection only vertices (oxygen atoms), while AlO_5 additionally uses two edges (Fig. 5b, c). The net has the unique topology, which has never been observed in crystal structures; we have deposited this topology in the *TopCryst* system (Shevchenko et al. 2022) under the name *dyp*1. The search in the databases of the *TopCryst* system revealed eight compounds. Among them, isotypic orthorhombic minerals cupromolybdite $Cu_3O[(Mo_{1.94}S_{0.06})O_4]_2$ (Zelenski et al. 2012) and vergasovaite $Cu_3O[(Mo,S)O_4SO_4]$ (Berlepsch et al. 1999) and synthetic solid solution series $[Cu_{(1-x)}Zn_x]_3O(MoO_4)_2$ (Reichelt et al. 2005) and $Zn_3O(MoO_4)_2$ (Hase et al. 2015). Further, there are isotypic monoclinic compounds $Zn_3O(MoO_4)_2$ (Söhnel et al. 1996) and $Zn_3O(SO_4)_2$ (Bald and Gruehn 1981) [the unit cell of the latter can be transformed to one close to that chosen for monoclinic $Zn_3O(MoO_4)_2$ using the matrix −1 0–1 / 0–1 0 / 0 0 1)] and glikinite $(Zn,Cu)_3O(SO_4)_2$ from the same Arsenatnaya fumarole (Nazarchuk et al. 2020), a natural Cu-bearing analogue of synthetic $Zn_3O(SO_4)_2$ (Bald and Gruehn 1981). All these sulfates and molybdates contain the nishanbaevite-like 6,6-coordinated layers as parts of the 3D framework structure. These layers are topologically close to the half of the double-layered core of the heteropolyhedral sheet in the nishanbaevite structure but differ from it in the ratio of tetrahedra and non-tetrahedral polyhedra and the presence of additional non-tetrahedral (five-fold or octahedral) polyhedra in zigzag chains. Besides glikinite, two minerals demonstrate some structural similarities with nishanbaevite, namely vergasovaite $Cu_3O(MoO_4)(SO_4)$ (Berlepsch et al. 1999) and cupromolybdite $Cu_3O(MoO_4)_2$ (Zelenski et al. 2012) isostructural to one another (Table 6). Their structural relationship with nishanbaevite (Figs. 3 and 4) is illustrated in Fig. 6. Notably, all these minerals originate from fumaroles of the Tolbachik volcano.

Table 4 Selected interatomic distances (Å) in the structure of nishanbaevite

A – O(7)	2.433(12)	Al(1) – O(5)	1.727(10)
- O(6)	2.478(15)	- O(3)	1.744(10)
- O(1)	2.762(8) x 2	- O(4)	1.756(9)
- O(6)	2.775(16)	- O(2)	1.965(7) x 2
- O(7)	3.152(18)	<Al(1) - O>	1.83
- O(7)	3.376(3) x 2	Al(2) – O(4)	1.800(3) x 2
<*A* - O>	2.89	- O(1)	1.881(7) x 2
As – O(3)	1.632(9)	- O(2)	2.058(6) x 2
- O(5)	1.656(9)	<Al(2) - O>	1.913
- O(2)	1.686(7) x 2		
<As - O>	1.665		
S – O(7)	1.433(8)		
- O(6)	1.448(8)		
- O(1)	1.482(7) x 2		
<S - O>	1.461		

Arsenate and sulfate tetrahedral anions are ordered in nishanbaevite. The As site contains admixed lighter constituents, S or/and Si and minor P (assumed based on EPMA data: see above). During structure refinement, they were formally considered together and designated as P' in Tables 2 and 3; scattering curve of P was used for P'. The sizes of AsO_4 tetrahedra with <As-O> 1.665 Å versus SO_4 tetrahedra with <S-O> 1.461 Å also confirm the As/S segregation in nishanbaevite. The similar As/S ordering in tetrahedral sites was also revealed in vasilseverginite $Cu_9O_4(AsO_4)_2(SO_4)_2$, another H-free sulfate-arsenate from the Arsenatnaya fumarole (Pekov et al. 2021).

The As/S ordering and the edge-sharing Al-polyhedra in nishanbaevite is similar to that in arsentsumebite $Pb_2Cu(AsO_4)(SO_4)(OH)$, a member of the brackebuschite supergroup (Zubkova et al. 2002). However, there is a partial As/S-ordering in arsentsumebite and the electronic contents in its tetrahedral

Table 5 Bond-valence calculations for nishanbaevite. Parameters were taken from Gagné and Hawthorne (2015)

	A	As	S	Al(1)	Al(2)	Σ
O(1)	$0.13^{\times 2\downarrow}$		$1.46^{\times 2\downarrow}$		$0.53^{\times 2\downarrow}$	2.12
O(2)		$1.21^{\times 2\downarrow}$		$0.43^{\times 2\downarrow}$	$0.34^{\times 2\downarrow}$	1.98
O(3)		1.41		0.75		2.16
O(4)				0.73	$0.65^{\times 2\downarrow\rightarrow}$	2.03
O(5)		1.32		0.79		2.11
O(6)	0.27 0.12		1.59			1.98
O(7)	0.29		1.65			
	0.05					2.05
	$0.03^{\times 2\downarrow\rightarrow}$					
Σ	1.05	5.15	6.16	3.13	3.04	

sites correspond to the occupation of $T1 = As_{0.63}S_{0.37}$ and $T2 = As_{0.37}S_{0.63}$. In common with arsentsumebite the double walls of nishanbaevite contain $M = M$-T chains, where $M = M$ means edge-sharing between M-polyhedra and M-T represents corner sharing between M-polyhedra and TO_4 tetrahedra (Eby and Hawthorne 1993).

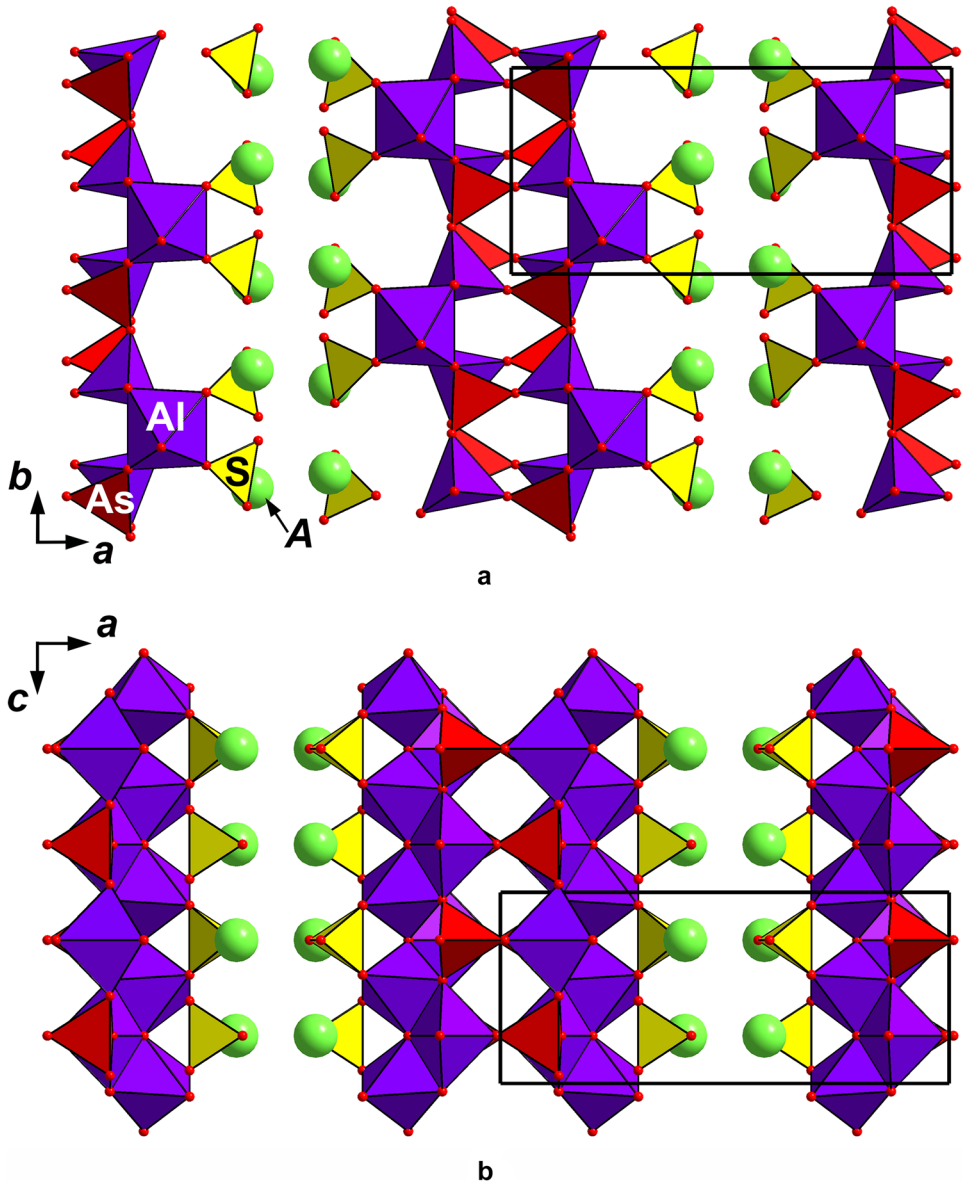

Fig. 3 The crystal structure of nishanbaevite in two projections. The unit cell is outlined

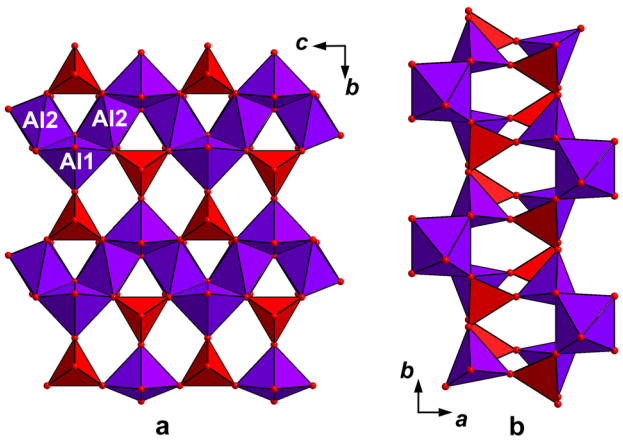

Fig. 4 A half of a double-layer core formed by Al-centred polyhedra and AsO_4 tetrahedra (**a**) and the double-layer core of the complicate sheet (**b**) in the structure of nishanbaevite

The crystal chemical features of the AsO_4-SO_4-ordered members of the alunite supergroup can be considered on the example of gallobeudantite $PbGa_3(AsO_4)(SO_4)(OH)_6$. In its structure distorted GaO_6 octahedra with shared vertices form the layers topologically related to those in so-called hexagonal bronzes. The octahedra occur at the vertices of a 6^3 kagome plane net, forming six-membered rings. At their junction there is a three-membered ring. Ordered AsO_4 and SO_4 tetrahedra are linked to these layers below and above in such a way that they are located on the same level respectively and are oriented along anti parallel directions (Jambor et al. 1996).

However, in most of arsenate-sulfates with As/S ordered structures the sulfate and arsenate tetrahedral groups perform a different function. In contrast with the acentric gallobeudantite (*R*3*m*), the disordered As/S distribution within the same tetrahedra was revealed in chemically related beudantite $PbFe^{3+}{}_3(AsO_4)(SO_4)(OH)_6$ with centrosymmetric structure (*R*-3 *m*). Both structures closely follow the the alunite-jarosite model (Szymański 1988; Giuseppetti and Tadini 1989). Oberwolfachite $SrFe^{3+}{}_3(AsO_4)(SO_4)(OH)_6$ with disordered As/S distribution is a new mineral of the beudantite group within the alunite supergroup which contain 10 and 53 mineral species, respectively (Chukanov et al. 2021).

The heteropolyhedral layer in the structure of sarmientite $Fe^{3+}{}_2(AsO_4)(SO_4)(OH)\cdot 5H_2O$ consists of the pairs of octahedral-tetrahedral $(Fe,As)O_n$-chains in which AsO_4 tetrahedra share all four O vertices with two nonequivalent Fe octahedra. The monodentate sulfate groups $[SO_4]$ play the role of the branches in these chains (Colombo et al. 2014). In nishanbaevite the heteropoyhedral (Al,As)-chains form the double layers. The SO_4 tetrahedra sharing vertices with $Al(2)O_6$ octahedra are suspended to the external parts of the layers and obviously play a subordinate role in these complexes.

The similar function of sulfate groups clearly appeared in bukovskýite $Fe_2(AsO_4)(SO_4)(OH)\cdot 9H_2O$ (Majzlan et al. 2012). The dominant feature of the structure of bukovskýite is the chains composed of Fe^{3+} octahedra and arsenate tetrahedra with the overall composition $Fe_2(AsO_4)(H_2O)_6(OH)$. Sulfate tetrahedra are located in the space between these chains and are linked to them by a network of H-bonds.

The heteropolyhedral layers formed by alternating corner-linked Al–O octahedra and acid-arsenate tetrahedra are the characteristic feature of juansilvaite $Na_5Al_3[AsO_3(OH)]_4[AsO_2(OH)_2]_2(SO_4)_2\cdot 4H_2O$ (Kampf et al. 2017). Isolated SO_4 tetrahedra are located in the interlayer region between these layers.

The dominant structural feature of chalcophyllite $Cu_9Al(AsO_4)_2(SO_4)_{15}(OH)_{12}\cdot 18H_2O$ is the arrangement of Cu and Al polyhedra into complex sheets. The As-centred tetrahedra are attached above and below these sheets by three vertices. The sheets are connected to each other by the hydrogen bonding system, where the sulfate groups are located in between (Sabelli 1980). According to (Sarp et al. 2014), the structure model of barrotite $Cu_9Al(HSiO_4)_2[(SO_4)(HAsO_4)_{0.5}](OH)_{12}\cdot 8H_2O$ contains the sheets topologically identical to chalcophyllite. They are also formed by Cu- and Al-centred polyhedra whereas AsO_4 tetrahedra in chalcophyllite are replaced by acidic $SiO_3(OH)$ tetrahedra in

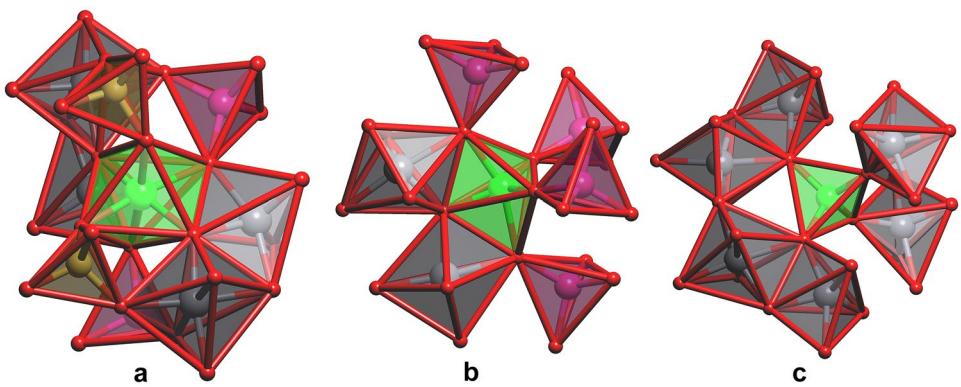

Fig. 5 Environment of AlO_6 octahedra (**a**), AlO_5 trigonal bipyramids (**b**) and AsO_4 tetrahedra (**c**) in nishanbaevite

Table 6 The framework Cu- and Zn-oxomolybdate and/or oxosulfate compounds with polyhedral units similar to the single sheets in the double layers of nishanbaevite

Compound / Mineral	Space group	Unit-cell parameters (Å,°)	*V*, Å^3	Reference
$Zn_3O(MoO_4)_2$	*Pnma*	7.629(1) 6.876(1) 14.573(1)	764.5	Hase et al. (2015)
$[Cu_{(1-x)}Zn_x]_3O(MoO_4)_2$	*Pnma*	7.6925(8) 6.9014(6) 14.5910(18)	774.6(1)	Reichelt et al. (2005)
x = 0.09		7.7022(5) 6.9160(6) 14.5485(11)	775.0(1)	
x = 0.18		7.7060(6) 6.9480(6) 14.4715(11)	774.8(1)	
x = 0.33		7.7337(5) 6.9860(6) 14.4536(11)	780.9(1)	
x = 0.48		7.7334(4) 7.0229(5) 14.4651(12)	785.6(1)	
x = 0.62		7.7493(5) 7.0615(6) 14.5020(10)	793.6(1)	
x = 0.76				
$Cu_3O[(Mo_{1.94}S_{0.06})O_4]_2$ cupromolybdite	*Pnma*	7.66380(10) 6.86700(10) 14.5554(2)	766.012(18)	Zelenski et al. (2012)
$Cu_3O[(Mo,S)O_4SO_4]$ vergasovaite	*Pnma*	7.421(2) 6.754(3) 13.624(5)	682.9	Berlepsch et al. (1999)
$Zn_3O(MoO_4)_2$	$P2_1/m$	7.7573(12) 7.1319(13) 8.370(2) 117.397(7)	411.1	Söhnel et al. (1996)
$Zn_3O(SO_4)_2$	$P2_1/m$	7.937(2) 6.690(2) 7.851(2) 124.39(1)*	344.0	Bald and Gruehn (1981)
$(Zn,Cu)_3O(SO_4)_2$ glikinite	$P2_1/m$	7.298(17) 6.588(11) 7.840(12) 117.14(3)	335.4(11)	Nazarchuk et al. (2020)
$(Zn,Cu)_3O(SO_4)_2$		7.3156(6) 6.6004(5) 7.8941(7) 117.424(5)	338.34(5)	Nekrasova et al. (2021)

*The cell could be transformed to a standardized one with $a = 7.365$, $b = 6.690$, $c = 7.851$ Å, $\beta = 117.213°$ by a matrix −1 0–1 / 0–1 0 / 0 0 1

barrotite. It is suggested that sulfate and arsenate tetrahedra in barrotite must occupy the interlayer space.

Leogangite $Cu_{10}(AsO_4)_4(SO_4)(OH)_6 \cdot 8H_2O$ (Lengauer et al. 2004) is another example which exhibits the topological difference between AsO_4 and SO_4 tetrahedra within the same structure. It contains the thick heteropolyhedral layers which are formed by the groups of five CuO_5 polyhedra (four distorted square pyramids + one distorted trigonal dipyramid) and AsO_4 tetrahedra. The sulfate tetrahedra link these layers to a loose framework.

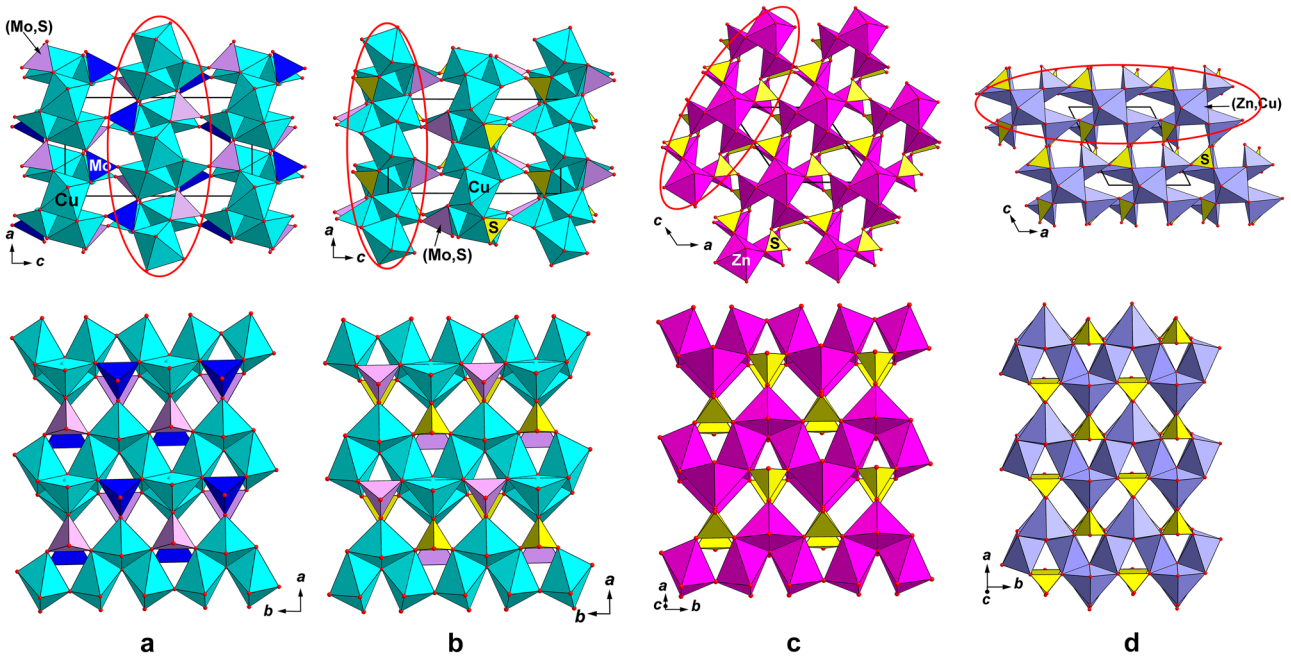

Fig. 6 The crystal structures (upper figures) and the fragments (shown by red ellipse) close to the half of the double layer in nishanbaevite (lower figures) in: cupromolybdite, drawn after Zelenski et al. (2012) (**a**); vergasovaite, drawn after Berlepsch et al. (1999) (**b**); synthetic $Zn_3O(SO_4)_2$, drawn after Bald and Gruehn (1981) (**c**) and its natural analogue glikinite, drawn after Nazarchuk et al. (2020) (**d**)

Thus, a large group of arsenate-sulfates exhibits the participation of AsO_4 tetrahedra in combination with cationic polyhedra in the heteropolyhedral complexes whereas SO_4 tetrahedra play a subordinate role in their structures. The different function of both AsO_4 and SO_4 tetrahedral groups is related with the closer values of thermochemical electronegativities between metal cations and As^{5+} vs. cations and S^{6+}. In particular, in nishanbaevite the difference of these values (Δ) between Al and As is 0.63 (Al 2.52 and As 3.15) whereas Δ between Al and S is 0.92 (Al 2.52 and S 3.44) (Tantardini and Oganov 2021).

Supplementary Information The online version contains supplementary material available at https://doi.org/10.1007/s00710-022-00803-0.

Acknowledgements SEM and EPMA studies were performed in Laboratory of Analytical Techniques of High Spatial Resolution, Department of Petrology, Moscow State University. This study was conducted using an XCalibur S CCD diffractometer (Moscow State University). The technical support by the Saint Petersburg State University X-Ray Diffraction Resource Center in the powder XRD study is acknowledged. We thank two anonymous referees and Editor Gerald Giester for valuable comments. The mineralogical studies, crystal structure determination and comparative crystal chemical analyses were supported by the Russian Science Foundation, grant no. 19-17-00050 to IVP, NVZ and DYP.

References

Agilent Technologies (2014) CrysAlisPro Software system, version 1.171.37.34. Agilent Technologies UK Ltd, Oxford, UK

Bald L, Gruehn R (1981) Die kristallstruktur von einem sulfat-reichen oxidsulfat des zinks. Naturwissenschaften 68:39 (in German)

Berlepsch P, Armbruster T, Brugger J, Bykova EY, Kartashov PM (1999) The crystal structure of vergasovaite $Cu_3O[(Mo,S)O_4SO_4]$, and its relation to synthetic $Cu_3O(MoO_4)_2$. Eur J Mineral 11:101–110

Blatov VA, Shevchenko AP, Proserpio DM (2014) Applied topological analysis of crystal structures with the program package ToposPro. Cryst Growth Des 14:3576–3586

Britvin SN, Dolivo-Dobrovolsky DV, Krzhizhanovskaya MG (2017) Software for processing the X-ray powder diffraction data obtained from the curved image plate detector of Rigaku RAXIS Rapid II diffractometer. Zapiski RMO 146(3):104–107 (in Russian)

Chukanov NV, Möhn G, Dal Bo F, Zubkova NV, Varlamov DA, Pekov IV, Chollet P, Vessely Ya, Jouffret L, Henot J-M, Friis H, Ksenofontov DA, Agakhanov AA, Britvin SN, Desor J, Koshlyakova NN, Pushcharovsky DYu (2021) Oberwolfachite, $SrFe^{3+}_3(AsO_4)(SO_4)(OH)_6$, a new alunite-supergroup mineral from the Clara mine, Schwarzwald, Germany and Monterniers mine, Rhône, France. Mineral Mag 85:808–816

Colombo F, Rius J, Vallcorba O, Pannunzio Miner EV (2014) The crystal structure of sarmientite, $Fe^{3+}_2(AsO_4)(SO_4)(OH)\cdot 5H_2O$, solved ab initio from laboratory powder diffraction data. Mineral Mag 78:347–360

Eby RK, Hawthorne FC (1993) Structural relations in copper oxysalt minerals. I. Structural hierarchy. Acta Crystallogr B49:28–56

Fedotov SA, Markhinin YK (eds) (1983) The great Tolbachik Fissure Eruption. Cambridge Univ. Press, New York

Gagné OC, Hawthorne FC (2015) Comprehensive derivation of bond-valence parameters for ion pairs involving oxygen. Acta Crystallogr B71:562–578

Giuseppetti G, Tadini C (1989) Beudantite: $PbFe_3(SO_4)(AsO_4)(OH)_6$, its crystal structure, tetrahedral site disordering and scattered Pb distribution. N Jb Mineral Mh 1989: 27–33

Hase M, Kuroe H, Pomjakushin VYu, Keller L, Tamura R, Terada N, Matsushita Y, Dönni A, Sekine T (2015) Magnetic structure of the spin-1/2 frustrated quasi-one-dimensional antiferromagnet $Cu_3Mo_2O_9$: appearance of a partial disordered state. Phys Rev B 92:054425

Jambor JL, Owens DR, Grice JD, Feinglos MN (1996) Gallobeudantite, $PbGa_3[(AsO_4),(SO_4)]_2(OH)_6$, a new mineral species from Tsumeb, Namibia, and associated new gallium analogues of the alunite-jarosite family. Can Mineral 34:1305–1315

Kampf AR, Nash BP, Dini M, Molina Donso AA (2017) Juansilvaite, $Na_5Al_3[AsO_3(OH)]_4[AsO_2(OH)_2]_2(SO_4)_2\cdot 4H_2O$, a new arsenate-sulfate from the Torrecillas mine, Iquique Province, Chile. Mineral Mag 81:619–628

Lengauer CL, Giester G, Kirchner E (2004) Leogangite, $Cu_{10}(AsO_4)_4(SO_4)(OH)_6\cdot 8H_2O$, a new mineral from the Leogang mining district, Salzburg province, Austria. Mineral Petrol 81:187–201

Majzlan J, Lazic B, Armbruster Th, Jonson MB, White MA, Fisher RA, Plasil J, Loun J, Skoda R, Novak M (2012) Crystal structure, thermodynamic properties, and paragenesis of bukovskýite, $Fe_2(AsO_4)(SO_4)(OH)\cdot 9H_2O$. J Mineral Petrol Sci 107:133–148

Nazarchuk EV, Siidra OI, Nekrasova DO, Shilovskikh VV, Borisov AS, Avdontseva EY (2020) Glikinite, $Zn_3O(SO_4)_2$, a new anhydrous zinc oxysulfate mineral structurally based on OZn_4 tetrahedra. Mineral Mag 84:563–567

Nekrasova DO, Siidra OI, Zaitsev AN, Ugolkov VL, Colmont M, Charkin DO, Mentré O, Chen R, Kovrugin VM, Borisov AS (2021) A fumarole in a one-pot: synthesis, crystal structure and properties of Zn- and Mg-analogs of itelmenite and a synthetic analog of glikinite. Phys Chem Minerals 48 Article number: 6

Pekov IV, Zubkova NV, Yapaskurt VO, Belakovskiy DI, Lykova IS, Vigasina MF, Sidorov EG, Pushcharovsky DYu (2014) New arsenate minerals from the Arsenatnaya fumarole, Tolbachik volcano, Kamchatka, Russia. I. Yurmarinite, $Na_7(Fe^{3+},mg,Cu)_4(AsO_4)_6$. Mineral Mag 78:905–917

Pekov IV, Koshlyakova NN, Zubkova NV, Lykova IS, Britvin SN, Yapaskurt VO, Agakhanov AA, Shchipalkina NV, Turchkova AG, Sidorov EG (2018) Fumarolic arsenates – a special type of arsenic mineralization. Eur J Mineral 30:305–322

Pekov IV, Britvin SN, Krivovichev SV, Yapaskurt VO, Vigasina MF, Turchkova AG, Sidorov EG (2021) Vasilseverginite, $Cu_9O_4(AsO_4)_2(SO_4)_2$, a new fumarolic mineral with a hybrid structure containing novel type of anion-centered tetrahedral structural units. Amer Mineral 106:633–640

Reichelt W, Steiner U, Söhnel T, Oeckler O, Duppel V, Kienle L (2005) Mischkristallbildung im system $Cu_3Mo_2O_9$ / $Zn_3Mo_2O_9$. Z Anorg Allg Chem 631:596–603 (in German)

Sabelli C (1980) The crystal structure of chalcophyllite. Zeit Krist - Crystalline Mater 151:129–140

Sarp H, Černy R, Puscharovsky DYu, Schouwink P, Teyssier J, Williams PA, Babalik H, Mari G (2014) La barrotite, $Cu_9Al(HSiO_4)_2[(SO_4)(HAsO_4)_{0.5}](OH)_{12}\cdot 8H_2O$, un nouveau minéral de la mine de Roua (Alpes-Maritimes, France). Riviera Scientifique 98:3–22

Shchipalkina NV, Pekov IV, Koshlyakova NN, Britvin SN, Zubkova NV, Varlamov DA, Sidorov EG (2020) Unusual silicate mineralization in fumarolic sublimates of the Tolbachik volcano, Kamchatka, Russia – Part 1: Neso-, cyclo-, ino- and phyllosilicates. Eur J Mineral 32:101–119

Söhnel T, Reichelt W, Oppermann H, Mattausch HJ, Simon A (1996) Zum system Zn/Mo/O. I. Phasenbestand und eigenschaften der

ternären zinkmolybdate; struktur von $Zn_3Mo_2O_9$. Z Anorg Allg Chem 622:1274–1280 (in German)

Tantardini C, Oganov AR (2021) Thermochemical electronegativities of the elements. Nat Commun 12:2087

Shevchenko AP, Blatov VA (2021) Simplify to understand: how to elucidate crystal structures? Struct Chem 32:507–519

Shevchenko AP, Shabalin AA, Karpukhin IYu, Blatov VA (2022) Topological representations of crystal structures: generation, analysis and implementation in the TopCryst system. STAM Methods 2(1):250–265

Siidra OI, Nazarchuk EV, Pautov LA, Borisov AS, Avdontseva EY (2021) Karlditmarite, IMA 2021-003. CNMNC Newsl 61; Mineral Mag 85:459–463

Sheldrick GM (2015) Crystal structure refinement with SHELXL. Acta Crystallogr –71:3–8

Symonds RB, Reed MH (1993) Calculation of multicomponent chemical equilibria in gas-solid-liquid systems: calculation methods, thermochemical data, and applications to studies of high-temperature volcanic gases with examples from Mount St. Helens. Amer J Scie 293:758–864

Szymański JT (1988) The crystal structure of beudantite, $Pb(Fe,Al)_3[(as,S)O_4]_2(OH)_6$. Can Mineral 26:923–932

Zelenski ME, Zubkova NV, Pekov IV, Polekhovsky YS, Pushcharovsky DY (2012) Cupromolybdite, $Cu_3O(MoO_4)_2$, a new fumarolic mineral from the Tolbachik volcano, Kamchatka Peninsula, Russia. Eur J Mineral 24(4):749–757

Zubkova NV, Pushcharovsky DYu, Giester G, Tillmanns E, Pekov IV, Kleimenov DA (2002) The crystal structure of arsentsumebite, $Pb_2Cu[(As,S)O_4]_2(OH)$. Mineral Petrol 75:79–88